

Enhancing Flood Risk Management: A Comparative Study of Regional Frequency Models in the Upper Meghna River, Bangladesh

ABSTRACT

Flood risk management is essential in Bangladesh, frequently affected by severe flooding due to its location at the confluence of the Ganges, Brahmaputra, and Meghna rivers. This study assesses the effectiveness of Gumbel and Log-Pearson Type III (LP3) probability distributions for flood frequency analysis at the Bhairab Bazar station in the Upper Meghna River. Using 32 years (1990-2021) of annual peak discharge data from the Bangladesh Water Development Board, flood magnitudes were predicted for various return periods. The Gumbel distribution predicted discharges from 10,709.71 m³/s for a 2-year return period to 24,519.62 m³/s for a 200-year return period, while LP3 estimates ranged from 10,701.51 m³/s to 22,911.84 m³/s for the same periods. The peak over threshold (POT) approach yielded higher discharge estimates, showing its sensitivity to extreme events. For a 200-year return period, the Gumbel-POT and LP3-POT estimates were 22,117.40 m³/s and 21,964.07 m³/s, respectively. Goodness-of-fit tests, including Kolmogorov-Smirnov, Anderson-Darling, and Chi-squared, favored the LP3 distribution for both extreme value series (EVS) and POT data, especially in critical tail regions. A rating curve was also developed using the generalized reduced gradient algorithm to better understand the river's hydraulic behavior. These findings are crucial for local flood management strategies. Discharges exceeding critical thresholds, like the 5.8-m danger level and 6.8-m severe flood level, highlight the need for robust measures. This analysis offers essential insights for designing hydraulic structures, planning flood mitigation, and improving prediction models to enhance flood risk assessments in the Upper Meghna River basin.

Keywords:Flood frequency analysis; rating curve; extreme value series; peak over threshold; flood risk management

1 INTRODUCTION

Flooding is a global hazard with devastating impacts, including loss of life, economic destruction, and widespread community disruption (Gaur & Simonovic, 2015; Yoshida et al., 2023). The risk of floods is exacerbated by climate change, which contributes to more intense rainfall and rising sea levels, thereby increasing flood risks (Hsiao et al., 2021). This underscores the need for robust flood risk management strategies, a necessity highlighted by Tanoue et al. (2016), who point to the escalating hazards posed by such environmental changes. This issue is particularly acute in Bangladesh, a nation uniquely vulnerable due to its geographical positioning at the confluence of three major rivers: the Ganges, Brahmaputra, and Meghna (Ghosh et al., 2023; Islam & Sharabony, 2023). Monsoon rains combined with snowmelt from upstream regions frequently cause these rivers to overflow, resulting in significant flooding events that have repeatedly struck the region (Alam et al., 2022). The geographical situation of Bangladesh, coupled with its high population density and an economy deeply reliant on agriculture—a sector highly susceptible to flooding—further intensifies its vulnerability.

Over the decades, Bangladesh has experienced numerous severe floods, with particularly disastrous events occurring in 1988, 1998, and 2007 (Hossen et al., 2022). These floods inundated large tracts of land, displaced millions of people, and led to substantial economic losses. For instance, the 1988 flood affected 61% of the country, rendering numerous people homeless and creating significant economic upheaval (Alexander & Wilson, 1995). The history of these catastrophic floods underscores the urgent necessity for enhanced flood management and mitigation strategies in the region. Historical data, such as that from England Jr et al. (2019), highlight the recurring nature of these flooding events, necessitating ongoing evaluation and enhancement of existing flood management practices.

Despite global and regional efforts to manage flood risks, the challenge remains formidable due to both natural and human-induced factors (Yoshida et al., 2021). Floods are the primary cause of deaths related to natural disasters globally, responsible for 6.8 million fatalities in the 20th century (Doocy et al., 2013). The number of individuals impacted by natural disasters has risen sharply, with the annual average increasing from 147 million in the 1980s to 211 million in the 1990s, with floods playing a significant role in this increase (Kreibich et al., 2015). Traditionally, structural measures like dams and levees have been central to mitigating flood impacts (Wenger,

2015). These strategies depend on accurate river flow predictions, achievable through comprehensive hydrological studies and flood frequency analysis. Flood frequency analysis helps estimate the likelihood of different magnitudes of flood events using various probability distributions based on historical discharge data, essential for designing hydraulic structures and flood forecasting (Tegegne et al., 2020).

The selection of probability distributions for flood frequency analysis has been a major research focus. Flood frequency analysis estimates flood magnitudes for various return periods, which is essential for designing hydraulic structures and planning flood mitigation measures (Tegegne et al., 2020). The fundamental premise is that past hydrological data can predict future flood events. Models such as the Generalized Extreme Value (GEV), Log-Pearson Type III (LP3), and Gumbel distributions are frequently used, though no single model has gained universal acceptance (Hanwatet al., 2020; Rao et al., 2022). The LP3 model, recommended by the United States Water Resources Council, is particularly valued for its ability to handle the significant skewness and kurtosis typical of peak flood data (Babee, 1975). In Bangladesh, limited research using empirical and hydrological models has traditionally favored the Gumbel and LP3 distributions for flood risk management (Alam et al., 2018). Nonetheless, there remains a persistent need for regional flood frequency analyses in this country.

The present study focuses on the Upper Meghna River, a less-researched but crucial area for Bangladesh's water resource management. Factors like urban expansion, wetland degradation, and infrastructural developments have heightened flood risks in its basin. Our research aims to address these challenges by evaluating the effectiveness of the Gumbel and LP3 distributions for flood frequency analysis in the Upper Meghna River across various return periods. The study compares these models and assesses the predicted discharge levels against severe flood levels identified by the Flood Forecasting & Warning Centre, Bangladesh Water Development Board (BWDB). This comparative analysis aims to assess the likelihood of floods exceeding critical thresholds, potentially leading to catastrophic overflows, and to provide essential insights for future flood planning and management initiatives.

2 STUDY SITE AND METHODOLOGY

2.1 Upper Meghna River Basin

The Upper Meghna River basin in Bangladesh is critical for flood risk management. The country, known for its extensive river systems, has over 7% of its land occupied by rivers. The Ganges-Brahmaputra-Meghna catchment spans 1.6 million km², with only 7.5% within Bangladesh, and the rest in India, China, Nepal, and Bhutan (Islam & Sharabony, 2023). The Meghna River catchment is the smallest, covering about 65,000 km², with 43% within Bangladesh, accounting for 24% of the country's territory (Masood & Takeuchi, 2016). The Meghna River, the largest waterway flowing into the Bay of Bengal, is vital for the region (Syed et al., 2018).

The Upper Meghna River basin, located in northeastern Bangladesh, features a variety of morphological elements, including alluvial ridges, natural levees, back swamps, haors, abandoned channels, oxbow lakes, and non-tidal plains. Bhairab Bazar station, situated in the Kishoreganj district (latitude: 24° 2' 44.088" N; longitude: 90° 59' 28.104" E), is crucial for understanding the basin's hydrology, as it drains a significant catchment area that receives water from various tributaries. The basin, bordered by the Garo Hills to the north and the Tripura Hills to the south, merges into the larger Meghna River system flowing towards the Bay of Bengal.

The Upper Meghna Basin's low-lying topography makes it prone to seasonal flooding during the monsoon from June to October, with annual rainfall averaging 1700 mm (Islam & Sharabony, 2023). Heavy rainfall and runoff from highlands lead to rapid water level increases, causing frequent and severe floods. Bhairab Bazar station is crucial for monitoring water levels and flood forecasting, providing vital historical data for managing flood risks. In addition, the basin's high population density and reliance on agriculture and fishing underscore the importance of effective flood management to protect livelihoods and well-being. The Upper Meghna River basin is essential for studying flood dynamics due to its geographical position, climatic conditions, and socioeconomic significance. Effective flood risk management in this basin is critical for protecting the local population's livelihoods.

2.2 Data collection and processing

This study analyzes flood frequency models for the Upper Meghna River in Bangladesh, focusing on annual peak flows recorded at the Bhairab Bazar station over a 32-year period

(1990-2021). The analysis assumes peak flows are independent and identically distributed (Orsini-Zegada and Escalante-Sandoval, 2016). Accurate flood frequency analyses depend on the quality and duration of recorded data, with potential inaccuracies leading to significant errors (Saghafian et al., 2014). Continuous data series of at least 30 years are recommended to minimize sampling errors and increase reliability (Holmes, 2014). Larger datasets generally provide more reliable estimates (Wright et al., 2020). The study utilizes discharge data from the BWDB, including daily water level and river discharge records, crucial for understanding flood dynamics and trends. The data was meticulously verified for accuracy and completeness. Initial processing involved cleaning the data by correcting outliers and filling missing values using interpolation methods.

Figure 3a presents time series graphs of daily observed discharges, highlighting significant trends and patterns over the 32-year period. These trends reveal notable inter-annual variability in peak discharge values, with extreme weather events influencing certain high flood years. Continuous and accurate data collection is emphasized for improving flood prediction models. In addition, Figure 3b illustrates the rating curve, which shows the relationship between discharge and river water level at the Bhairab Bazar station. This curve was developed using the generalized reduced gradient algorithm (Zakwan & Ara, 2022), resulting in a stable and predictable relationship with a coefficient of determination (R^2) value of 0.602. This stability is crucial for accurate flood forecasting and management. The steepness of the curve indicates a high sensitivity of river stage to discharge changes, which is vital for flood risk assessment and infrastructure planning.

For the flood frequency analysis, the dataset was divided into the extreme value series (EVS) and the peak over threshold (POT) series. The EVS includes the maximum annual discharge values from 1990 to 2021, while the POT series includes discharge values exceeding a predefined threshold, representing moderate to severe flood events. By selecting 32 significant peaks for the POT series, the study captures a comprehensive range of over-threshold flood events. This dual approach enhances the robustness of the flood frequency analysis by capturing the full spectrum of flood events, from extreme annual floods to frequent moderate floods. The study provides insights crucial for designing effective flood management and mitigation strategies tailored to the specific flood dynamics of the Upper Meghna River.

2.3 Probability distribution models

To analyze the flood frequency of the Upper Meghna River, we utilized two commonly applied probability distribution models: the Gumbel model (Gumbel, 1958) and LP3 model (Pearson, 1916). These models are represented by equations (1) through (13).

2.3.1 Gumbel probability distribution

The Gumbel distribution serves as a statistical model for extreme events, especially in regionalization procedures. It is considered a suitable method for predicting flood recurrence intervals (e.g., Samantaray & Sahoo, 2020). The reduced variate (Y_t) for a given return period (T) is determined using the following formula:

$$Y_t = - [\ln \{ \ln (T/(T-1)) \}] \quad (1)$$

The reduced mean (Y_n) and reduced standard deviation (S_n) are obtained from the Gumbel distribution table for the given sample size (number of recorded years) (Gumbel, 1958). The frequency factor (K_t) is then estimated using:

$$K_t = \frac{(Y_t - Y_n)}{S_n} \quad (2)$$

where K_t is the frequency factor, Y_t is the reduced variate, Y_n is the reduced mean, and S_n is the reduced standard deviation. The predicted discharge is computed using the standard normal distribution formula for various return periods:

$$Q_p = \mu + K_t \sigma \quad (3)$$

where Q_p is the predicted discharge (m^3/s), μ is the mean, and σ is the standard deviation.

2.3.2 Log-Pearson Type III (LP3)

The Log-Pearson Type III (LP3) distribution is a statistical approach employed to model frequency distribution values, particularly for predicting floods at specific locations. Also referred to as the three-parameter Gamma distribution (Millington et al., 2011; Samantaray & Sahoo, 2020), it has been extensively utilized in flood frequency analysis since its endorsement by the Water Resources Council of the United States (Singh & Singh, 1998). This distribution is especially effective for analyzing flood peak data.

To implement the LP3 model, the logarithm of the actual discharges (Z) is first calculated, followed by determining the logarithmic mean (μ) and logarithmic standard deviation (σ):

$$Z = \log_{10}Q \quad (4)$$

Subsequently, the coefficient of skewness (C_s) is computed using the logarithmic discharges (Z). For a given return period (T), the probability (P) is then calculated as follows:

$$P = \frac{1}{T} (\%) \quad (5)$$

Using the standard normal distribution table, we interpolated to find the standard normal deviate (z). The frequency factor (K_t), which depends on the coefficient of skewness (C_s) and the return period (T) (Lane, 2002), is adjusted using the formula proposed by Kite (1977):

$$K_t = z + (z^2 - 1)k + \frac{1}{3}(z^3 - 6z)k^2 - (z^2 - 1)k^3 + zk^4 + \frac{1}{3}k^5 \quad (6)$$

$$\text{where, } k = \frac{C_s}{6} \quad (7)$$

The predicted logarithmic discharge is calculated as:

$$q_p = \mu + K_t\sigma \quad (8)$$

where q_p is the predicted logarithmic discharge. The predicted discharge (Q_p) in m^3/s is then obtained by taking the antilog of q_p (Subramanya, 2017):

$$Q_p = \text{antilog}(q_p) \quad (9)$$

2.4 Goodness of fit test

The suitability of these distributions for a specific study can be evaluated using various statistical techniques, such as goodness of fit tests (Church, 1983). These tests assist in identifying the most appropriate probability distribution method rather than simply discarding others (Millington et al., 2011). They assess the difference between observed and expected values derived from the applied distributions. We employed the following three goodness of fit tests:

2.4.1 Anderson- Darling (A-D)

This test evaluates the fit of an observed cumulative distribution function (CDF) against an expected CDF, placing additional emphasis on the tails of the distribution (Samantaray& Sahoo, 2020):

$$D^2 = -m - \frac{1}{m} \sum_{j=1}^m (2j - 1) \times [\ln F(y_j) + \ln(1 - F(y_{m-j+1}))] \quad (10)$$

2.4.2 Kolmogorov–Smirnov (K-S) test

The Kolmogorov–Smirnov (K-S) test evaluates the alignment of probability distribution methods, suitable even for small sample sizes. It checks if a sample originates from a specified continuous probability distribution using the empirical cumulative distribution function (CDF) (Samantaray& Sahoo, 2020):

$$F_m(y) = \frac{1}{m} \times [\text{observation number} \leq y] \quad (11)$$

The test statistic (K) is the maximum vertical distance between the hypothetical and empirical CDFs:

$$K = \max_{1 \leq j \leq m} (F(y_j) - \frac{j-1}{m}, \frac{j}{m} - F(y_j)) \quad (12)$$

2.4.3 Chi-squared test

The chi-squared test assesses whether a sample is drawn from a population with a specified distribution. It utilizes binned data, and the value of the test statistic depends on the binning. Pearson (1916) recommended using the chi-squared (χ^2) distribution for this test (Samantaray& Sahoo, 2020):

$$\chi^2 = \sum_{j=1}^l \frac{(O_j - E_j)^2}{E_j} \quad (13)$$

where O_j is the observed frequency, j is the number of observations, and E_j (the expected frequency) is calculated as $F(Y_2) - F(Y_1)$, with F being the cumulative distribution function, l being $1 + \log_2 m$, and m being the sample size.

3 RESULTS AND DISCUSSION

3.1 Flood frequency estimates for various return periods

Estimating flood frequency for various return periods is essential for effective flood risk management. A comparative analysis of flood frequency models for the Upper Meghna River at Bhairab Bazar station offers valuable insights. Table 1 shows predicted discharges for return periods from 2 to 200 years using the Gumbel distribution. For the EVS data series, discharges start at 10,709.71 m³/s for a 2-year return period and rise to 24,519.62 m³/s for a 200-year return period. The POT data series predicts higher discharges, starting at 14,397.00 m³/s for a 2-year return period and reaching 22,117.40 m³/s for a 200-year return period. These higher values from the POT series indicate its effectiveness in capturing more extreme flood events, which is crucial for estimating higher discharges for longer return periods (Phillips et al., 2018).

Similarly, Table 2 provides flood frequency estimates using the LP3 distribution. For the EVS series, the discharge for a 2-year return period is 10,701.51 m³/s, increasing to 22,911.84 m³/s for a 200-year return period. The POT series estimates start at 14,265.76 m³/s for a 2-year return period and rise to 21,964.07 m³/s for a 200-year return period. The LP3 distribution, known for better handling skewed data (Gogoi & Patnaik, 2023), shows that the POT series yields higher discharge estimates for shorter return periods but slightly lower estimates for longer return periods compared to the Gumbel distribution. This variance highlights the importance of selecting the appropriate distribution model based on data characteristics and specific flood risk management needs (Rahman et al., 2013).

Figure 4 compares the estimated flood discharges using both the Gumbel and LP3 distributions for EVS and POT data. High coefficients of determination (R^2) for both distributions indicate a good fit to the observed data. However, discrepancies in predicted discharges, particularly for higher return periods, highlight the importance of model selection. The POT data series consistently predicts higher discharges compared to the EVS series across both distributions, indicating its sensitivity to recent extreme events. This is critical for near-term flood risk management, while the EVS method provides more conservative estimates over longer periods, offering stable long-term risk assessments (Binh et al., 2019).

Integrating both EVS and POT approaches could enhance flood risk management strategies. Short-term infrastructure planning could benefit from POT estimates, while long-term policies and land-use planning could rely on EVS estimates. The study underscores the POT method's

capability to account for extreme flood events, making it a potentially more reliable tool for regions prone to high variability in flood magnitudes. For example, the 200-year return period discharge using the Gumbel distribution is 24,519.62 m³/s (EVS) versus 22,117.40 m³/s (POT), and for the LP3 distribution, it is 22,911.84 m³/s (EVS) versus 21,964.07 m³/s (POT). These findings align with previous studies emphasizing the variability in flood frequency estimates based on distribution models and data series (Hu et al., 2020). Ultimately, this study highlights the importance of using multiple flood frequency models and data series to capture a range of potential flood discharges. The choice of method should be tailored to the specific needs of flood risk management, balancing short-term responsiveness with long-term reliability.

3.2 Goodness of fit test

Table 3 displays the results of the K-S, A-D, and Chi-squared goodness-of-fit tests for the Gumbel and LP3 distributions using EVS and POT data. For the EVS data, the K-S test statistic for the Gumbel distribution is 0.07323 with a p-value of 0.99049, indicating no rejection of the null hypothesis at the 0.05 significance level. Similarly, the LP3 distribution shows a test statistic of 0.0757 and a p-value of 0.98636, also indicating no rejection of the null hypothesis. These results suggest a slightly better fit for the Gumbel distribution according to the K-S test, though the differences are marginal. The A-D test results support these findings, with the Gumbel distribution showing a statistic of 0.2045 and the LP3 distribution slightly better at 0.19797, both of which do not reject the null hypothesis. This consistency across tests is essential for validating our model selection. Additionally, the Chi-squared test results align with this trend, showing non-significant statistics of 0.3772 for Gumbel and 0.36097 for LP3 at the 0.05 level. For the POT data, the LP3 distribution is slightly favored. The K-S test statistic for the Gumbel distribution is 0.14596 with a p-value of 0.45999, while the LP3 distribution has a lower test statistic of 0.11999 and a higher p-value of 0.7017. The A-D test and Chi-squared test results show a similar pattern, indicating the LP3 distribution has a marginally better fit for the POT data as well.

Figures 6 and 7 provide visual comparisons of the CDF and probability-probability (P-P) plots for the Gumbel and LP3 distributions with both EVS and POT data. The CDF plots in Figure 5 demonstrate that both distributions fit the EVS data well, with the LP3 distribution showing a slightly better fit in the tail regions, which are critical for flood risk management. The P-P plots

in Figure 6 further confirm these findings, as the points for both distributions closely follow the 45-degree line, indicating a good fit. Notably, the LP3 distribution exhibits less deviation from this line, particularly for the POT data, suggesting a superior overall fit compared to the Gumbel distribution.

The slight edge of the LP3 distribution over the Gumbel distribution in both EVS and POT data suggests its suitability for flood frequency analysis in the Upper Meghna River. This finding aligns with previous studies that have highlighted the LP3 distribution's ability to better capture the skewness and kurtosis of hydrological data (Reinders & Munoz, 2024). The robustness of our findings is further supported by the consistent non-rejection of the null hypothesis across all goodness-of-fit tests, underscoring the reliability of the LP3 distribution for flood risk management applications. Furthermore, the superior performance of the LP3 distribution in the tail regions is critical for managing extreme flood events, which are of primary concern in risk management strategies (Rizwan et al., 2018). Accurate modeling of these tail events can lead to improved preparedness and mitigation strategies, ultimately reducing the potential impacts of floods on communities in the Upper Meghna River basin.

3.3 Comparison of flood frequency estimates with severe flooding threshold

The analysis compares flood frequency estimates with critical water levels as defined by local authorities, specifically the BWDB. The danger level is set at a 5.8-m water level, while the severe flooding threshold is marked at 6.8 m. These benchmarks are crucial for assessing the risk and potential impact of flooding on the Upper Meghna River region. Figure 7 illustrates the predicted discharges for different return periods and their relation to these critical water levels. The discharge values corresponding to these water levels were obtained using the rating curve presented in Figure 3b, which maps the relationship between observed discharge and river water level at the targeted hydrological monitoring station.

For shorter return periods, such as 2 years, the predicted discharges indicate a relatively modest increase in water levels. These levels generally remain above the danger threshold (5.8 m or approximately 10,150 m³/s, as shown in Figure 3b) but below or around the severe flooding threshold (6.8 m or approximately 13,036 m³/s, as shown in Figure 3b). Specifically, this 2-year return period reflects a discharge just above normal river levels, indicating minimal risk to the surrounding areas. As we progress to the 5-year return period, the predicted discharge begins to

approach the danger level, highlighting an increasing risk of severe flooding that necessitates vigilant monitoring and early warning systems. In contrast, longer return periods, such as 10, 25, 50, 100, and 200 years, predict significantly higher discharges that exceed the severe flooding threshold of 6.8 m. These longer return periods indicate a potential for catastrophic flooding events. For instance, the 100-year return period predicts a discharge well above 10 m of water level, signifying extreme flood events that could severely impact infrastructure and communities. These results underscore the necessity for robust flood management strategies to mitigate the impacts of such rare but devastating events. This aligns with previous studies that emphasize the importance of incorporating long-term flood frequency data into risk management frameworks (Šakić Trogrlić et al., 2022;).

From the perspective of hydraulic structure design, our findings suggest the imperative to construct embankments, levees, and floodwalls that can handle the maximum predicted discharges for the highest return periods. Specifically, these structures need to be designed with additional height and strength to accommodate the worst-case scenarios as identified by the 200-year return period data. Regular maintenance and inspections are also crucial to ensure these structures remain effective over time, particularly in the face of wear and potential damage from frequent flooding events. In addition to the design and maintenance of hydraulic structures, the study emphasizes the importance of river dredging to increase the water carrying capacity. This measure can help mitigate the impact of floods by allowing larger volumes of water to flow through the river channel without breaching the danger thresholds. From a risk management perspective, the study highlights the importance of incorporating these flood frequency estimates into urban and rural planning processes. By understanding the probabilities and magnitudes of potential flood events, local authorities and planners can better allocate resources and implement proactive measures to protect communities and infrastructure.

4 FUTURE RESEARCH DIRECTIONS

The current study identifies several critical areas for future research to improve flood risk management in the Upper Meghna River basin, Bangladesh. Key priorities include incorporating advanced hydrological and climate models to enhance flood prediction accuracy, with high-resolution climate projections essential for assessing future flood risks under various climate change scenarios (Tanoue et al., 2016; Hsiao et al., 2021). Developing sophisticated predictive

models and comprehensive multi-model approaches that integrate both EVS and POT methods is crucial for understanding and predicting flood risks in diverse hydrological contexts (Phillips et al., 2018). In addition, utilizing geographic information systems and remote sensing technologies can significantly enhance flood monitoring and management, offering continuous monitoring of water levels and land use changes for real-time flood prediction (Islam et al., 2022; Islam et al., 2023). Integrating these technologies with traditional hydrological data can create a comprehensive flood risk assessment framework (Masood & Takeuchi, 2016).

Research should also explore the socio-economic impacts of flooding and the effectiveness of various mitigation strategies. Mixed-methods approaches should assess structural and non-structural mitigation measures, such as floodplain zoning and community-based flood management (Kreibich et al., 2015; Hossen et al., 2022). Developing early warning systems that combine local knowledge with scientific data is critical for enhancing community resilience (Islam & Sharabony, 2023). Moreover, longitudinal studies tracking the effectiveness of flood management interventions over time are necessary to understand different strategies' performance under varying conditions, offering insights for adaptive management practices (Wright et al., 2020; Hu et al., 2020). Evaluating the performance of existing flood mitigation infrastructure and investigating nature-based solutions can provide co-benefits for biodiversity and ecosystem services (Wenger, 2015).

Finally, policy-oriented research is essential to develop comprehensive flood risk management frameworks aligned with national and regional development plans. Collaborative efforts among governments, research institutions, and international organizations are crucial for addressing flood risk management challenges in the Upper Meghna River basin (Ghosh et al., 2023). Addressing these research directions will enable more resilient and adaptive flood management strategies, mitigating the negative impacts of flooding on communities and ecosystems.

5 CONCLUSION

The comparative analysis of regional frequency models for flood risk management in the Upper Meghna River basin reveals important insights. Evaluating the Gumbel and Log-Pearson Type III (LP3) probability distributions using data from the Bhairab Bazar station highlights the need for precise flood prediction models to inform local strategies. The Gumbel distribution predicted higher discharges for extreme flood events, especially using the peak over threshold (POT)

approach, indicating higher sensitivity to extreme events. In contrast, the LP3 distribution, supported by goodness-of-fit tests, effectively captured the skewness typical of flood data, particularly in the tail regions. The findings suggest that the LP3 distribution provides a marginally better fit for both extreme value series (EVS) and POT data, which is crucial for robust flood risk management. Predicted discharges for various return periods indicate the potential for severe flooding events, exceeding critical thresholds set by local authorities. This analysis is vital for designing hydraulic structures, planning flood mitigation measures, and improving prediction models. Additionally, integrating advanced hydrological and climate models and continuous data collection is recommended to enhance flood risk assessments. Combining EVS and POT approaches can offer a comprehensive understanding of flood risks, balancing short-term responsiveness with long-term reliability. These findings support policy formulation and the development of resilient infrastructural and non-structural measures to mitigate flood impacts in the Upper Meghna River basin.

DATA AVAILABILITY STATEMENT

Data supporting the study's findings are not publicly available. However, they can be obtained from the corresponding author upon reasonable request.

REFERENCES

- Alam MA, Emura K, Farnham C, Yuan J. Best-fit probability distributions and return periods for maximum monthly rainfall in Bangladesh. *Climate*. 2018; 6(1):9.
Available: <https://doi.org/10.3390/cli6010009>
- Alam S, Jahan S, Noor F. The surface water system, flood and water resources management of Bangladesh. *Bangladesh Geosciences and Resources Potential*. 2022; 467-546.
- Alexander TW, Wilson GL. Technique for estimating the 2-to 500-year flood discharges on unregulated streams in rural Missouri. US Department of the Interior, US Geological Survey; 1995.
- Binh LT, Umamahesh NV, Rathnam EV. High-resolution flood hazard mapping based on nonstationary frequency analysis: case study of Ho Chi Minh City, Vietnam. *Hydrological Sciences Journal*. 2019;64(3):318-35.

Available:<https://doi.org/10.1080/02626667.2019.1581363>

Bobee B. The log Pearson type 3 distribution and its application in hydrology. *Water resources research*. 1975;11(5):681-689.

Available:<https://doi.org/10.1029/WR011i005p00681>

Church M. Pattern of instability in a wandering gravel bed channel. *Modern and ancient fluvial systems*. 1983; 169-80.

Available:<https://doi.org/10.1002/9781444303773.ch13>

Doocy S, Daniels A, Murray S, Kirsch TD. The human impact of floods: a historical review of events 1980-2009 and systematic literature review. *PLoS currents*. 2013;5.

Available:<http://dx.doi.org/10.1371/currents.dis.f4deb457904936b07c09daa98ee8171a>

England Jr JF, Cohn TA, Faber BA, Stedinger JR, Thomas Jr WO, Veilleux AG, Kiang JE, Mason Jr RR. Guidelines for determining flood flow frequency—Bulletin 17C. US Geological Survey; 2019.

Available:<https://doi.org/10.3133/tm4B5>

Gaur A, Simonovic SP. Projected changes in the dynamics of flood hazard in the Grand River Basin, Canada. *International Journal of Environment and Climate Change*. 2015; 5 (1):37-51.

Available:<https://doi.org/10.9734/BJECC/2015/17705>.

Ghosh S, Roy S, Islam A, Shit PK, Datta DK, Islam MS, Das BC. Floods of Ganga-Brahmaputra-Meghna Delta in Context. In *Floods in the Ganga–Brahmaputra–Meghna Delta*. 2023; 1-17. Cham: Springer International Publishing.

Available:https://doi.org/10.1007/978-3-031-21086-0_1

Gogoi P, Patnaik SK. Flood Frequency Analysis of Jiadhhal River Basin, India using Log Pearson Type III Distribution Method. *The Asian Review of Civil Engineering*. 2023;12(1):6-9.

Available:<https://doi.org/10.51983/tarce-2023.12.1.3565>

Gumbel EJ. *Statistics of extremes*. Columbia university press. 1958.

Lane, B. (2002). *Statistical methods in hydrology* (Vol. 496). Iowa state press, Iowa.

- Hanwat S, Pal K, Panda KC, Sharma G, Mandloi S, Tripathi V. Flood frequency analysis for BurhiGandak River Basin. *International Journal of Environment and Climate Change*. 2020; 10(6):82-89.
Available:<https://doi.org/10.9734/ijecc/2020/v10i630207>
- Holmes RR. Floods: Recurrence intervals and 100-year floods (USGS). 2014.
Available:<http://www.water.usgs.gov/edu/>
- Hossen MN, Nawaz S, Kabir MH. Flood Research in Bangladesh and Future Direction: an insight from last three decades. *International Journal of Disaster Risk Management*. 2022;4(1):15-41.
Available:<https://doi.org/10.18485/ijdrm.2022.4.1.2>
- Hsiao SC, Chiang WS, Jang JH, Wu HL, Lu WS, Chen WB, Wu YT. Flood risk influenced by the compound effect of storm surge and rainfall under climate change for low-lying coastal areas. *Science of the total environment*. 2021;764:144439.
Available:<https://doi.org/10.1016/j.scitotenv.2020.144439>
- Hu L, Nikolopoulos EI, Marra F, Anagnostou EN. Sensitivity of flood frequency analysis to data record, statistical model, and parameter estimation methods: An evaluation over the contiguous United States. *Journal of Flood Risk Management*. 2020;13(1):e12580.
Available:<https://doi.org/10.1111/jfr3.12580>
- Islam MS, Sharabony A. Characteristics of Flood in the Meghna River Basin Within Bangladesh. *InFloods in the Ganga–Brahmaputra–Meghna Delta 2023*; 423-447. Cham: Springer International Publishing.
Available:https://doi.org/10.1007/978-3-031-21086-0_18
- Islam MT, Yoshida K, Nishiyama S, Sakai K. Mutual validation of remote hydraulic estimates and flow model simulations using UAV-borne LiDAR and deep learning-based imaging techniques. *Results in Engineering*. 2023;20:101415.
Available:<https://doi.org/10.1016/j.rineng.2023.101415>
- Islam MT, Yoshida K, Nishiyama S, Sakai K, Adachi S, Pan S. Promises and uncertainties in remotely sensed riverine hydro-environmental attributes: Field testing of novel

- approaches to unmanned aerial vehicle-borne lidar and imaging velocimetry. *River Research and Applications*. 2022;38(10):1757-74.
Available: <https://doi.org/10.1002/rra.4042>
- Kite GW. Frequency and risk analyses in hydrology. *Water Resources Publications*. 1977;224.
- Kreibich H, Bubeck P, Van Vliet M, De Moel H. A review of damage-reducing measures to manage fluvial flood risks in a changing climate. *Mitigation and adaptation strategies for global change*. 2015;20:967-89.
Available: <https://doi.org/10.1007/s11027-014-9629-5>
- Masood M, Takeuchi K. Climate change impacts and its implications on future water resource management in the Meghna Basin. *Futures*. 2016;78:1-8.
Available: <https://doi.org/10.1016/j.futures.2016.03.001>
- Millington N, Das S, Simonovic SP. The comparison of GEV, log-Pearson type 3 and Gumbel distributions in the Upper Thames River watershed under global climate models. *Water Resources Research Report*. 2011. Department of Civil and Environmental Engineering, The University of Western Ontario London, Ontario, Canada.
- Orsini-Zegada L, Escalante-Sandoval C. Flood frequency analysis using synthetic samples. *Atmósfera*. 2016;29(4):299-309.
Available: <https://doi.org/10.20937/ATM.2016.29.04.02>
- Pearson K. XLII. on a brief proof of the fundamental formula for testing the goodness of fit of frequency distributions, and on the probable error of "P.". *The London, Edinburgh, and Dublin Philosophical Magazine and Journal of Science*. 1916;31(184):369-78.
Available: <https://doi.org/10.1080/14786440408635509>
- Phillips RC, Samadi SZ, Meadows ME. How extreme was the October 2015 flood in the Carolinas? An assessment of flood frequency analysis and distribution tails. *Journal of Hydrology*. 2018;562:648-63.
Available: <https://doi.org/10.1016/j.jhydrol.2018.05.035>

Rahman AS, Rahman A, Zaman MA, Haddad K, Ahsan A, Imteaz M. A study on selection of probability distributions for at-site flood frequency analysis in Australia. *Natural hazards*. 2013;69:1803-13.

Available:<https://doi.org/10.1007/s11069-013-0775-y>

Rao PS, Ramana MV, Reddy KM, Kumar AA. Flood Frequency Analysis of Araniar Medium Irrigation Project in Chittoor District by using Gumbel's Distribution. *International Journal of Environment and Climate Change*. 2022; 12(10):538-44.

Available:<https://doi.org/10.9734/ijecc/2022/v12i1131004>

Reinders JB, Munoz SE. Accounting for hydroclimatic properties in flood frequency analysis procedures. *Hydrology and Earth System Sciences*. 2024;28(1):217-27.

Available:<https://doi.org/10.5194/hess-28-217-2024>

Rizwan M, Guo S, Xiong F, Yin J. Evaluation of various probability distributions for deriving design flood featuring right-tail events in pakistan. *Water*. 2018;10(11):1603.

Available:<https://doi.org/10.3390/w10111603>

Saghafian B, Golian S, Ghasemi A. Flood frequency analysis based on simulated peak discharges. *Natural Hazards*. 2014;71:403-17.

Available:<https://doi.org/10.1007/s11069-013-0925-2>

Šakić Trogrlić R, van den Homberg M, Budimir M, McQuistan C, Sneddon A, Golding B. Early warning systems and their role in disaster risk reduction. In *Towards the “perfect” weather warning: bridging disciplinary gaps through partnership and communication* 2022; 11-46. Cham: Springer International Publishing.

Available:https://doi.org/10.1007/978-3-030-98989-7_2

Samantaray S, Sahoo A. Estimation of flood frequency using statistical method: Mahanadi River basin, India. *h2oj*. 2020;3(1):189-207.

Available:<https://doi.org/10.2166/h2oj.2020.004>

Singh VP, Singh VP. Log-pearson type III distribution. Entropy-based parameter estimation in hydrology. 1998; 252-74.

Available:https://doi.org/10.1007/978-94-017-1431-0_15

- Subramanya K. Engineering hydrology. McGraw-Hill, New Delhi; 2017.
- Syed ZH, Choi G, Byeon S. A numerical approach to predict water levels in ungauged regions—
Case study of the meghna river estuary, Bangladesh. *Water*. 2018;10(2):110.
Available: <https://doi.org/10.3390/w10020110>
- Tanoue M, Hirabayashi Y, Ikeuchi H. Global-scale river flood vulnerability in the last 50 years.
Scientific reports. 2016;6(1):36021.
Available: <https://doi.org/10.1038/srep36021>
- Tegegne G, Melesse AM, Asfaw DH, Worqlul AW. Flood frequency analyses over different
basin scales in the Blue Nile River basin, Ethiopia. *Hydrology*. 2020;7(3):44.
Available: <https://doi.org/10.3390/hydrology7030044>
- Wenger C. Better use and management of levees: reducing flood risk in a changing climate.
Environmental Reviews. 2015;23(2):240-55.
Available: <https://doi.org/10.1139/er-2014-0060>
- Wright DB, Yu G, England JF. Six decades of rainfall and flood frequency analysis using
stochastic storm transposition: Review, progress, and prospects. *Journal of Hydrology*.
2020;585:124816.
Available: <https://doi.org/10.1016/j.jhydrol.2020.124816>
- Yoshida K, Kajikawa Y, Nishiyama S, Islam MT, Adachi S, Sakai K. Three-dimensional
numerical modelling of floods in river corridor with complex vegetation quantified using
airborne LiDAR imagery. *Journal of Hydraulic Research*. 2023;61(1):88-108.
Available: <https://doi.org/10.1080/00221686.2022.2106596>
- Yoshida K, Nagata K, Maeno S, Mano K, Nigo S, Nishiyama S, Islam MT. Flood risk
assessment in vegetated lower Asahi River of Okayama Prefecture in Japan using
airborne topo-bathymetric LiDAR and depth-averaged flow model. *Journal of Hydro-
Environment Research*. 2021;39:39-59.
Available: <https://doi.org/10.1016/j.jher.2021.06.005>

Zakwan M, Ara Z. Establishing sediment rating curves using optimization technique. In River and Coastal Engineering: Hydraulics, Water Resources and Coastal Engineering 2022; 1-8. Cham: Springer International Publishing.

Available: https://doi.org/10.1007/978-3-031-05057-2_1

FIGURE WITH LEGENDS

UNDER PEER REVIEW

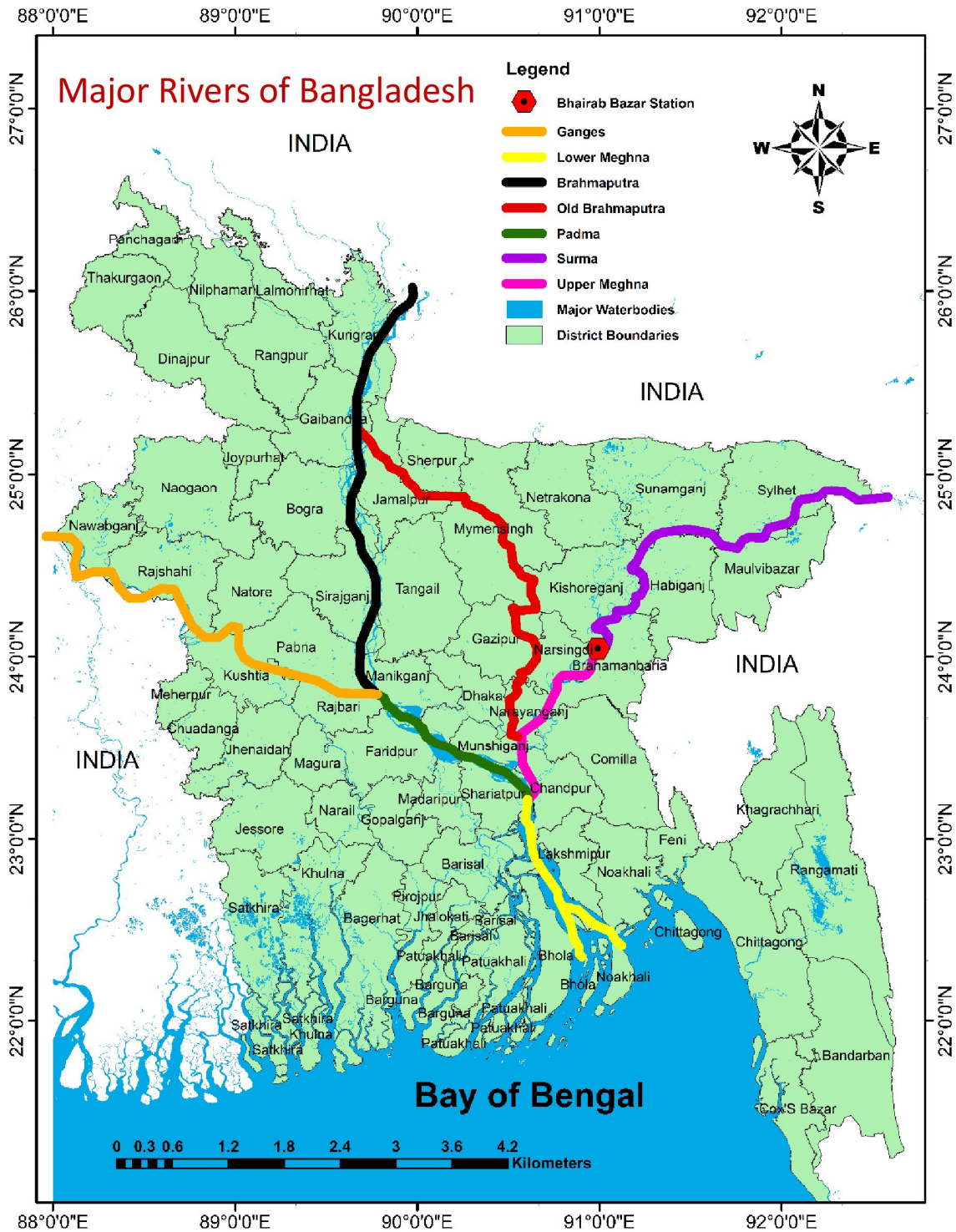


FIGURE 1 Map displaying the major rivers of Bangladesh, with focus on the Bhairab Bazar station along the Upper Meghna River.

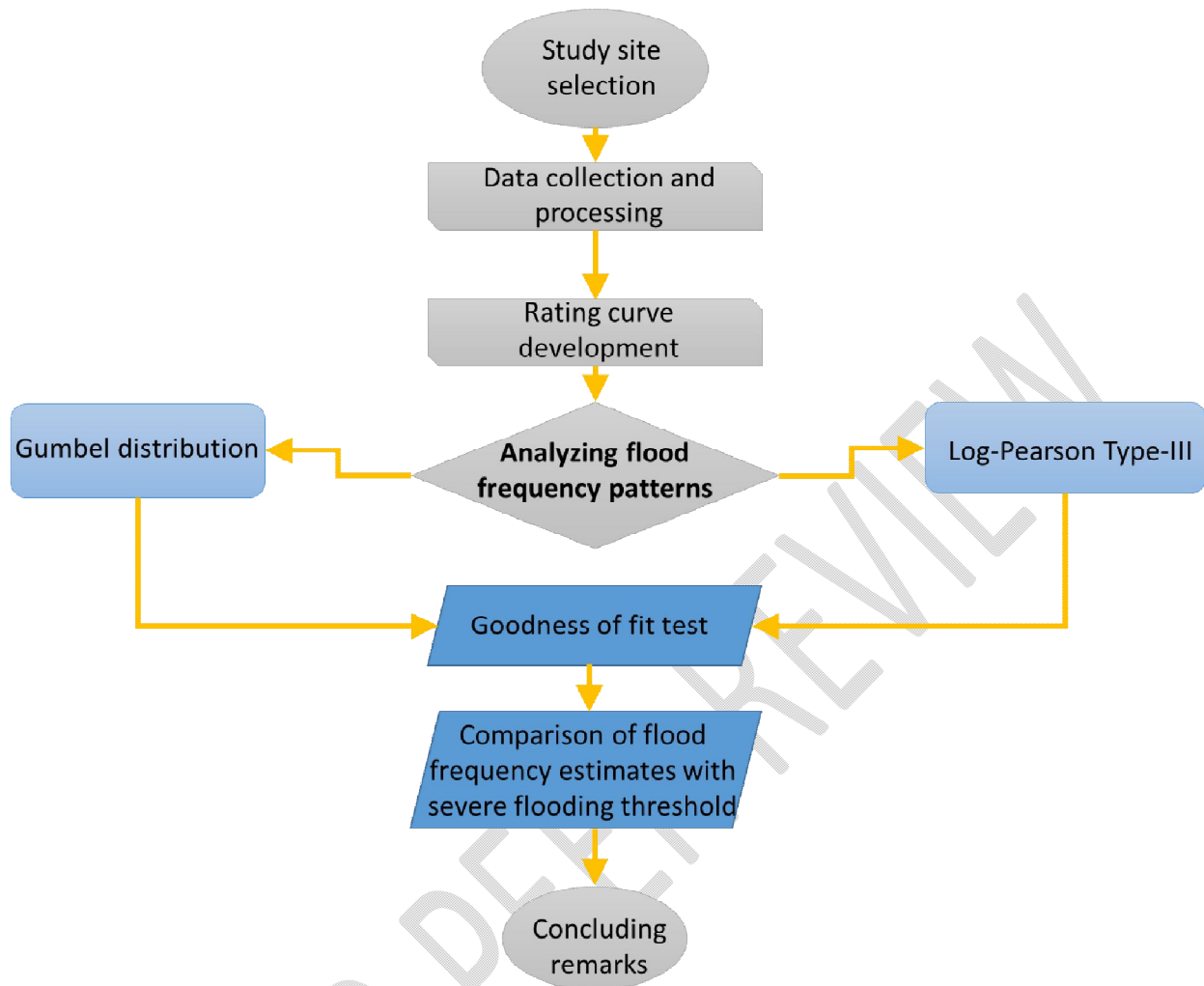


FIGURE 2 Flowchart outlining the methodologies employed in this study.

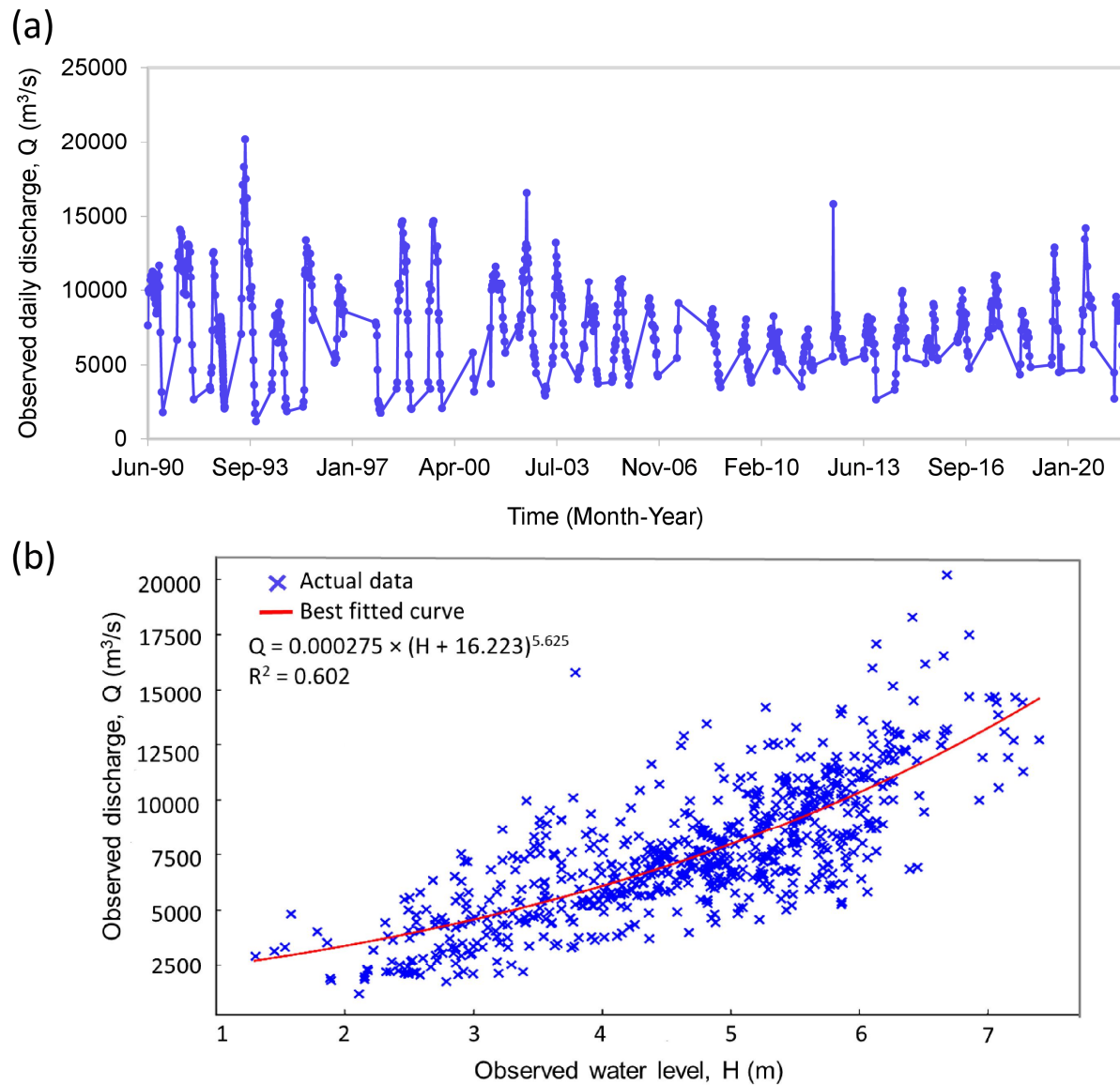


FIGURE 3 (a) Time series plots depicting discharges over 32 years (1990-2021), and (b) rating curve illustrating observed discharge versus river water level (or stage) at the Bhairab Bazar station along the Upper Meghna River in Bangladesh.

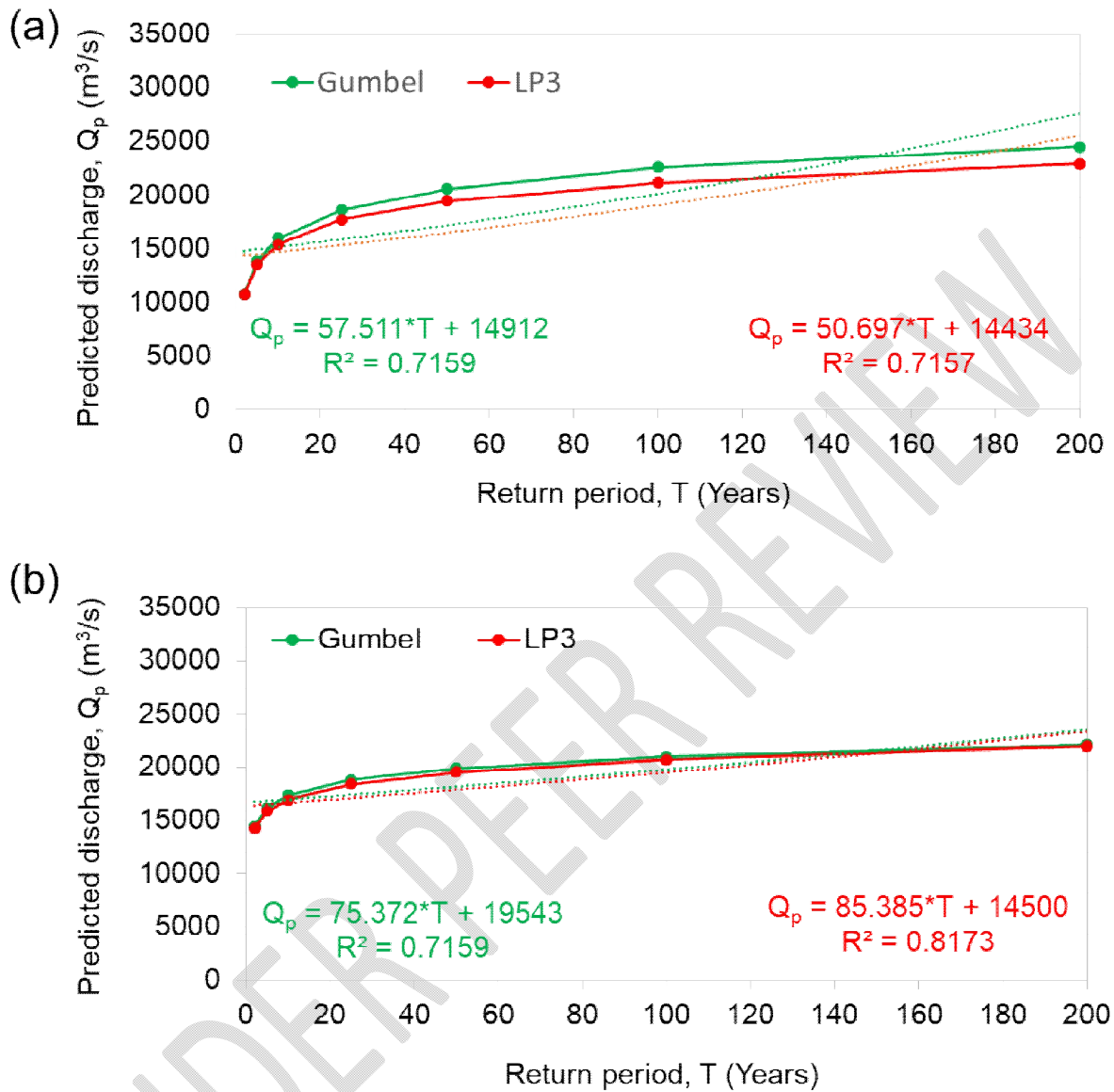


FIGURE 4 Comparative analysis of estimated flood discharges using Gumbel and Log-Pearson Type III (LP3) distributions with (a) extreme value series (EVS) and (b) peak over threshold (POT) data.

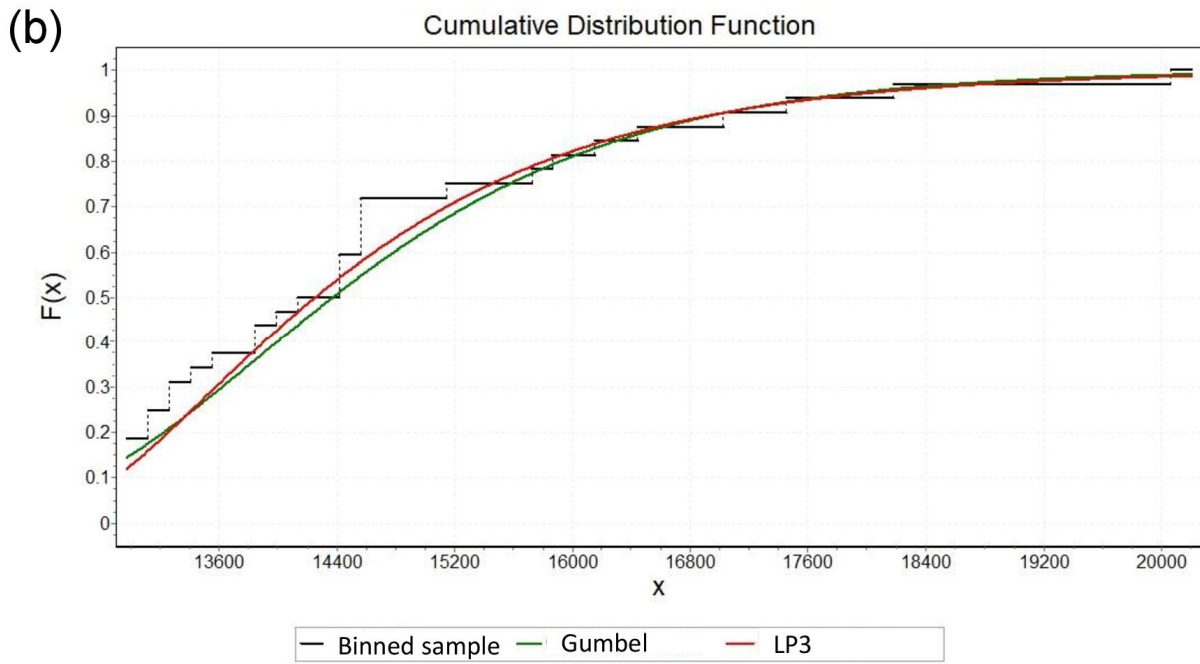
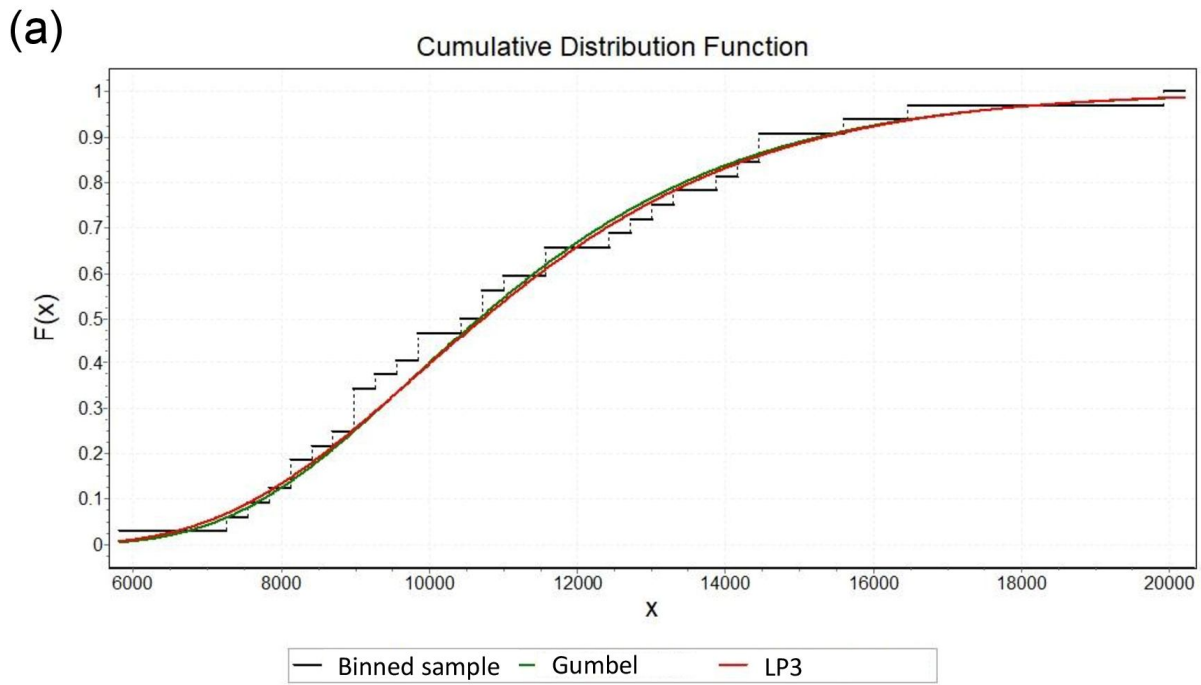


FIGURE 5 Cumulative distribution function comparison of Gumbel and Log-Pearson Type III distributions for (a) extreme value series (EVS) and (b) peak over threshold (POT) data.

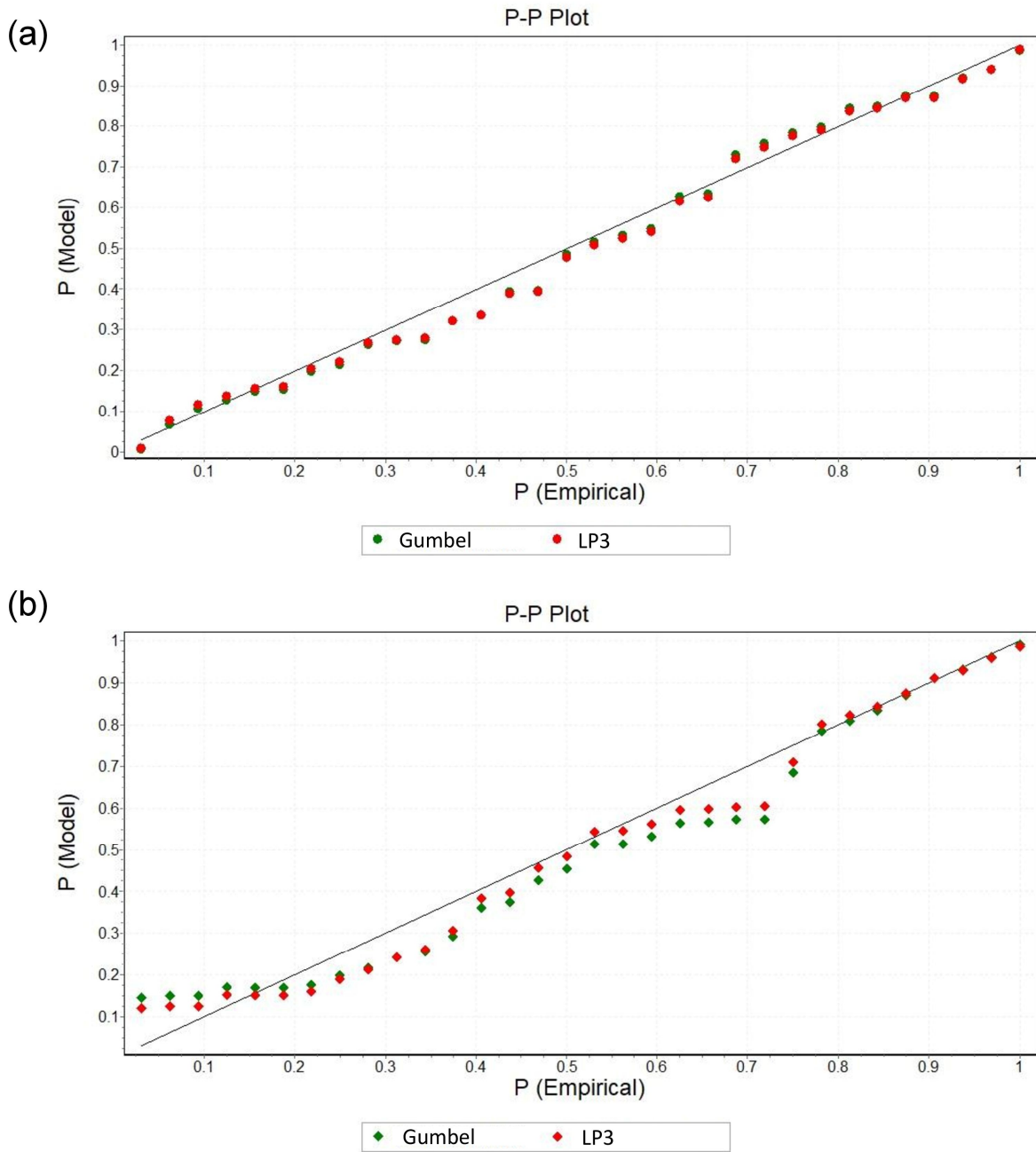


FIGURE 6 Probability-Probability (P-P) plot assessing distribution fitting for Gumbel and Log-Pearson Type III (LP3) distributions with (a) extreme value series (EVS) and (b) peak over threshold (POT) data.

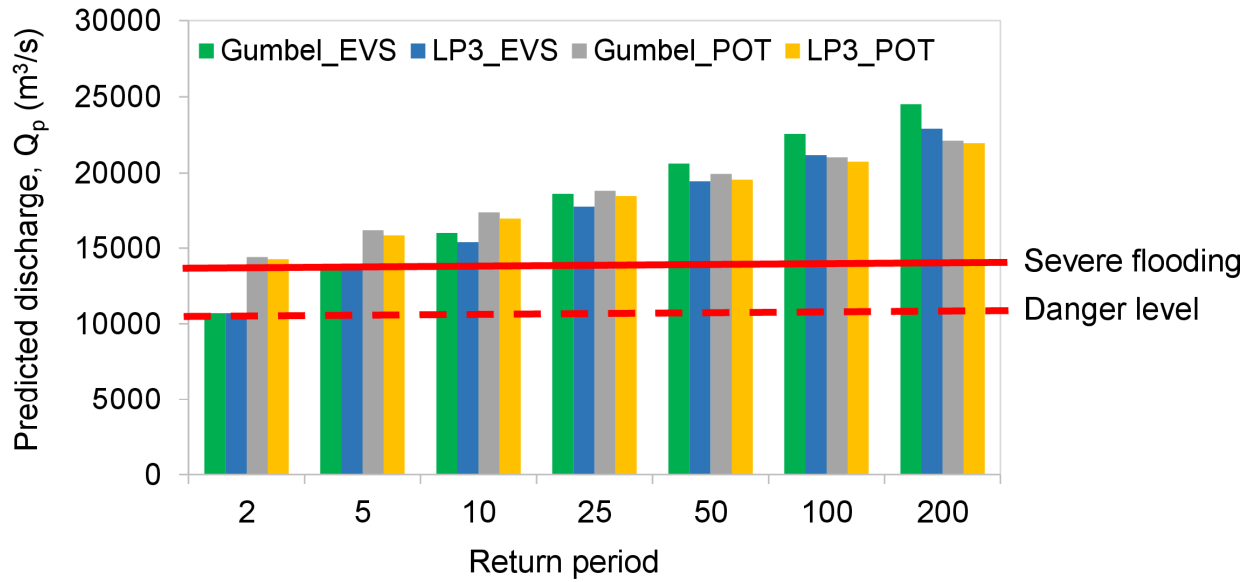


FIGURE 7 Comparison of flood frequency estimates with the danger level (5.8 m water level) and severe flooding threshold (6.8 m water level) set by local authorities. The discharge values for these thresholds were derived from the rating curve shown in Figure 3b.

TABLE 1 Flood frequency estimates for Bhairab Bazar station along the Upper Meghna River in Bangladesh using Gumbel distribution with extreme value series (EVS) and peak over threshold (POT) data series.

Return period (T) in years	Reduced variate, Y_t	Frequency factor, K_t	Predicted discharge, Q_p in m^3/s	
			EVS	POT
2	0.37	-0.15	10709.71	14397.00
5	1.50	0.86	13885.11	16172.20
10	2.25	1.53	15987.51	17347.54
25	3.20	2.38	18643.89	18832.59
50	3.90	3.01	20614.55	19934.28
100	4.60	3.63	22570.65	21027.83
200	5.30	4.25	24519.62	22117.40

TABLE 2 Flood frequency estimates of Bhairab Bazar station at Upper Meghna River of Bangladesh using Log-Pearson Type III distribution with extreme value series (EVS) and peak over threshold (POT) data series.

Return period (T) in years	Frequency factor, K_t		Predicted logarithmic discharge, q_p in m^3/s		Predicted discharge, Q_p in m^3/s	
	EVS	POT	EVS	POT	EVS	POT
2	-0.03	-0.19	4.03	4.15	10701.51	14265.76
5	0.84	0.74	4.13	4.20	13568.75	15833.15
10	1.3	1.34	4.19	4.23	15383.32	16934.61
25	1.82	2.09	4.25	4.27	17728.42	18419.81
50	2.16	2.63	4.29	4.29	19451.81	19569.17
100	2.47	3.15	4.33	4.32	21168.74	20743.69
200	2.76	3.66	4.36	4.34	22911.84	21964.07

TABLE 3 Goodness of fit test results for Gumbel and Log-Pearson Type III (LP3) distributions with extreme value series (EVS) and peak over threshold (POT) data.

Data Series	Distribution	Kolmogorov–Smirnov (K-S) (critical value at 0.05 = 0.23424)				Anderson–Darling (A-D) (critical value at 0.05 = 2.5018)			Chi-squared (critical value at 0.05 = 7.814)			
		Statistic	P-Value	Reject	Rank	Statistic	Reject	Rank	Statistic	P-Value	Reject	Rank
EVS	Gumbel	0.07323	0.99049	No	1	0.2045	No	2	0.3772	0.94491	No	2
	LP3	0.0757	0.98636	No	2	0.19797	No	1	0.36097	0.94818	No	1
POT	Gumbel	0.14596	0.45999	No	2	0.72069	No	2	1.4953	0.68336	No	2
	LP3	0.11999	0.7017	No	1	0.49299	No	1	1.3846	0.70915	No	1